

## Research Article

# Nonlinear Time-History Analysis for Validation of the Displacement-Based Seismic Assessment of the RC Upper Bridge of a Dam

P. Lestuzzi <sup>1,2</sup>, H. Charif,<sup>3</sup> S. Rossier,<sup>4</sup> M. Ferrière,<sup>5</sup> and J.-P. Person<sup>5</sup>

<sup>1</sup>Résonance Ingénieurs-Conseils SA, Carouge, Switzerland

<sup>2</sup>EPFL-ENAC-IIC-IMAC, Lausanne, Switzerland

<sup>3</sup>Sollertia, Monthey, Switzerland

<sup>4</sup>SCIA, Herk-de-Stad, Belgium

<sup>5</sup>CNR Ingénierie, Lyon, France

Correspondence should be addressed to P. Lestuzzi; [pierino.lestuzzi@epfl.ch](mailto:pierino.lestuzzi@epfl.ch)

Received 8 March 2018; Revised 7 June 2018; Accepted 25 June 2018; Published 22 July 2018

Academic Editor: Pier Paolo Rossi

Copyright © 2018 P. Lestuzzi et al. This is an open access article distributed under the Creative Commons Attribution License, which permits unrestricted use, distribution, and reproduction in any medium, provided the original work is properly cited.

The seismic assessment of a secondary structure of the Chancy-Pougny dam, namely, the upper bridge, is discussed in this paper. A first seismic assessment, performed according to classical force-based methodology, concluded the necessity of an extensive retrofitting for the upper bridge. By contrast, the application of the displacement-based approach showed that the current situation is already satisfactory, and therefore, practically no retrofitting is needed. The paper focuses on the nonlinear time-history analyses which were achieved in order to check the accuracy of the results obtained using the displacement-based method. The structural characteristics of the reinforced concrete upper bridge are similar to those of conventional bridges. However, the piers were built with very little reinforcement and consequently they will exhibit a rocking behavior in case of earthquake loading. Rocking is rather a favorable failure mechanism and is related to a certain amount of displacement capacity. However, this behavior is not linked to plastic energy dissipation which may significantly increase the related displacement demand. In order to determine the real displacement demand, nonlinear time-history analyses were achieved with SDOF systems defined by an “S” shape hysteretic model. Spectrum compatible stationary synthetic accelerograms and slightly modified recorded earthquakes were both used for acceleration time-histories. The results showed that the displacement demand corresponds well with the one determined by usual push-over analysis. The results show a very favorable seismic situation, related to a relatively stiff structure associated to rock soil conditions with an A class soil. The seismic safety of the upper bridge is already satisfactory for the current state (without retrofitting). Consequently, the proposed costly reinforcement for the upper bridge could be significantly reduced.

## 1. Introduction

In the field of earthquake engineering, the popularity of displacement-based analysis is steadily increasing for both design of new structures and assessment of existing structures. Compared to traditional force-based methods, displacement-based methodology is more closely related to the real seismic behavior and therefore provides much more accurate results. Moreover, the results are generally more favorable than the corresponding ones for classical force-based methods, for example [1]. As a consequence, the

displacement-based method provides a very valuable tool for the seismic assessment of existing structures because it may save expensive retrofitting [2]. This paper reports an example of extreme cost reduction obtained thanks to the application of the displacement-based method.

Traditional force-based methodologies, such as the equivalent force method or the response spectrum method, are based on simplified elastic analyses to determine seismic action, for example [3]. They intentionally avoid the use of more elaborate analysis to account for postelastic behavior. More precisely, they use the so-called “behavior



FIGURE 1: (a) General view of the Chancy-Pougny hydropower development scheme [8]. (b) View of the part of the upper dam starting from the cable tower with the three identical piers I, II, and III and their “elephant feet” at the base [10].

factor” for this purpose. The behavior factor is a global strength reduction factor, mainly based on the famous “equal displacement rule,” and is specified in the construction standards. The displacement-based methodology was proposed in the 1990s [4] and is now well established for seismic design and assessment of reinforced concrete and steel structures. This methodology is also proposed for the seismic assessment of unreinforced masonry structures [5]. Moreover, recent research efforts are oriented towards the application of rocking structures for the design of bridge piers, mainly in association with post-tensioning for example [6, 7]. For existing structures, the main advantage of displacement-based analysis consists of considering realistic structural elements which were not properly designed and detailed according to seismic requirements. Note that the “behavior factor” does not belong to the displacement-based methodology. In fact, displacement-based analysis may be considered as a way to determine the actual value of the behavior factor related to the investigated structure.

The Chancy-Pougny hydropower development scheme, located on the French-Swiss Rhone border, is a gate structure dam made of masonry and reinforced concrete. In the framework of renewing the concession, the investigation of the seismic behavior of the dam was requested by the supervisory bodies. This paper concerns the seismic assessment of a partial structure of the Chancy-Pougny dam, namely, the upper bridge. A first seismic assessment, performed according to classical force-based methodology, concluded to the necessity of a huge retrofitting for the upper bridge. By contrast, the application of the displacement-based approach showed that the current situation is already satisfactory and therefore practically no reinforcements are needed. As the involvement of the displacement-based method in the context of dam engineering is not usual (to the best knowledge of the authors, it was the first time), the supervisory authorities requested additional investigations in order to validate the obtained results. After a brief description of the force-based analysis, the related initial proposed retrofitting and the performed displacement-based assessment, the paper focuses on the nonlinear time-history analysis which was achieved in the framework of the project in order to check the accuracy of the results obtained by push-over analysis.

*1.1. Brief Description of the Chancy-Pougny Dam.* The Chancy-Pougny hydropower development scheme is located on the French-Swiss Rhone border near Geneva (Figure 1). It is a gate structure dam made of masonry and reinforced concrete constructed in 1925 to supply Schneider plants in Le Creusot (France). Its main characteristics are a head of 10 m, 4 bays equipped with Stoney type gates with 12 m openings, one bay with a reservation for a future lock, a tower and an upper bridge to carry the cables from the plant to a power substation, and a partial lower bridge [8, 9].

In the framework of renewing the exploitation concession, the French-Swiss supervisory authorities (i.e., Direction Régionale de l’Environnement, de l’Aménagement et du Logement (DREAL) and Swiss Federal Office of Energy (OFEN)) requested the owner of the structure (the Société des Forces Motrices de Chancy-Pougny (SFMCP)), to carry out a detailed investigation of the dynamic behavior of the dam under seismic loading. Note that architectural constraints should be additionally considered because the plant is classified as a historic monument.

*1.2. Characteristics of the Upper Bridge.* Five concrete piles support the equipments (Figure 2). They are composed of lower pillars, 21.7 m high, made of reinforced concrete with stone facing, and upper piers, 12.4 m high, made of lightly reinforced concrete with cement coating. The piles are founded on caissons sunk into a sand stone (molasse) substratum. An intermediate 4 m thick foundation slab protects the dam against hydraulic erosion between piles.

A 26 m high cable tower is used to route the electrical power cables from the plant to the substation: a gallery in the upper bridge completes this routing between the two banks, more precisely between the cable tower and the right abutment (Figure 1). The upper bridge is approximately 115 m long and is made of a series of beams, simply supported at the top of the five piers, called pier I to pier V (from the cable tower to the right abutment). The distance between the piers is about 15.5 m for piers I to IV (Figure 3) and is increased to 22.7 m for pier V.

The cable tower has a rectangular hollow cross section with a length of 7.5 m and a width of 4.9 m (Figure 4). The thickness of the walls of the cable tower is about 0.8 m. The cross section of the piers is nearly rectangular. The length is 6.8 m and the width is 2.7 m for piers I, II, and III (Figure 4)

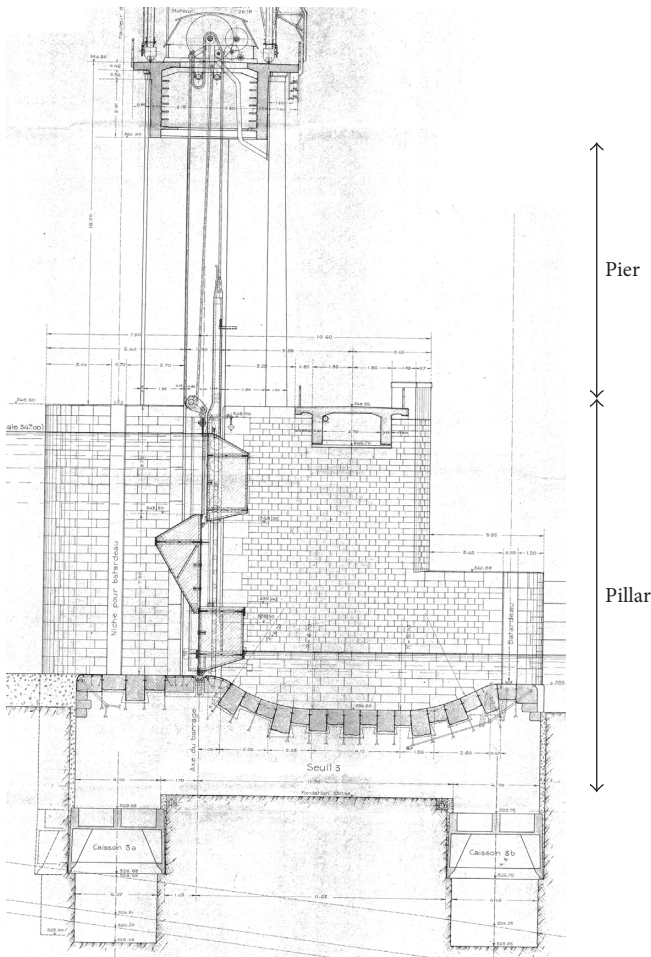


FIGURE 2: Cross section of the Chancy-Pougny dam.

and 3.2 m for piers IV and V. Except for the lower 1.9 m at the base, the piers are solid. At the base, piers I, II, and III are hollowed in the middle along the section's axes for operational purposes. As a consequence, the base of these identical piers is practically reduced to a group of four squat columns, called "elephant feet" (Figure 4). The cross section of the squat column at the base is about 1 m to 2 m. Piers IV and V are similar but with hollow cross section instead of "elephant feet" at the base. The deck of the upper bridge is composed of a series of 6 reinforced concrete beams with hollow cross sections and a height of 3.6 m.

**1.3. Seismic Parameters.** The seismic assessment of the dam is performed according to the OFEN requirements. Given the characteristics of the development scheme, the dam is classified into a class II dam according to the Swiss classification [11]. Consequently, an earthquake loading with a return period of 5000 years should be taken into account. For a 5% damping ratio and soil class A (rock conditions), the corresponding response spectrum is characterized by a peak ground acceleration of 0.23 g and a maximum plateau acceleration of 0.58 g horizontally (Figure 5).

Soil class A:  $S=1.0$  (-);  $T_B=0.10$  (s);  $T_C=0.40$  (s);  $T_D=3.00$  (s).

## 2. Force-Based Seismic Analysis

The first approach consisted of a linear dynamic analysis using the response spectrum method. The OFEN response spectrum was applied in the two main horizontal directions and in the vertical direction with the prescribed attenuation factor of 2/3. The entire structure was modeled with three-dimensional finite elements (Figure 6), taking into account dynamic soil-structure interaction (mixed rock-alluvial soil foundations) and the structure-mass of entrained water interaction.

The obtained results showed that the main deficiencies appear in the cross-stream direction which is not mobilized under service conditions. Excess tensile stresses (up to 10 MPa) were determined in the cable tower and upper part of the pillars due to cross-stream excitation. For the lower part of the pillars, conventional tensile resistance was also exceeded due to entrained water in the along-stream direction. Concerning the upper bridge, due to the very light reinforcement of the piers, the results showed that the strength at the base of the piers was far exceeded in both directions (cross-stream and along-stream).

**2.1. Initial Proposed Retrofitting.** The initially adopted methodology leads to a major retrofitting project that is also complex in terms of feasibility, particularly for long drilled tensioned anchors in old concrete structures. For the pillars, the proposed retrofitting includes several anchors coupled with injections to improve the concrete quality.

For the upper bridge, the initial proposed retrofitting consisted of St Andrew steel cross braces to resist cross-stream excitation (Figure 7). In addition, vertical anchors were proposed for the piers to prevent cracking at the base.

## 3. Displacement-Based Approach, "Push-Over" Analysis

At this stage, in order to limit the retrofitting, an alternative approach was proposed to the supervisory authorities. This alternative approach is based on a "push-over" analysis of the upper bridge. Experimental investigations have shown that reinforced concrete with low reinforcement is not necessarily associated with very poor seismic behavior, for example [12]. This method may obviously not be applied to the lower part of the dam because of its role in hydraulic retention.

The structural characteristics of the upper bridge are similar to the ones of conventional bridges. Therefore it was proposed to apply modern displacement-based seismic assessment methodologies (usually involved in existing structures) to the upper bridge.

In the case of the Chancy-Pougny dam, the displacement-based approach allows the consideration of the rocking behavior of the 12.4 m high piers of the upper bridge. This means that, compared to the initial force-based approach, the condition of avoiding cracking at the base of the piers is no longer considered. By contrast, cracking at the base is used since it leads to a seismically satisfactory rocking behavior, generally associated with a relatively large displacement

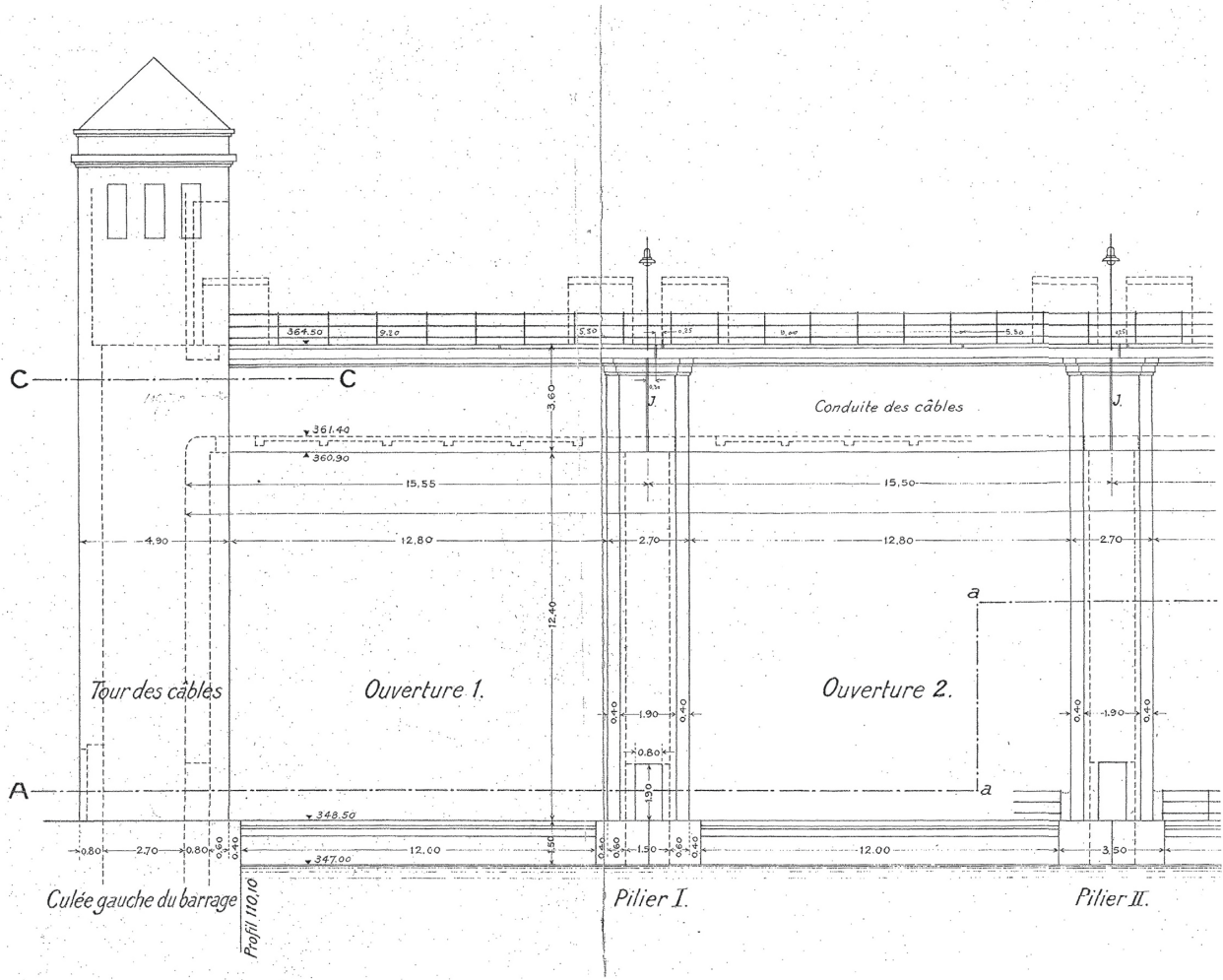


FIGURE 3: View of the cable tower and the piers I and II of the Chancy-Pouigny dam.

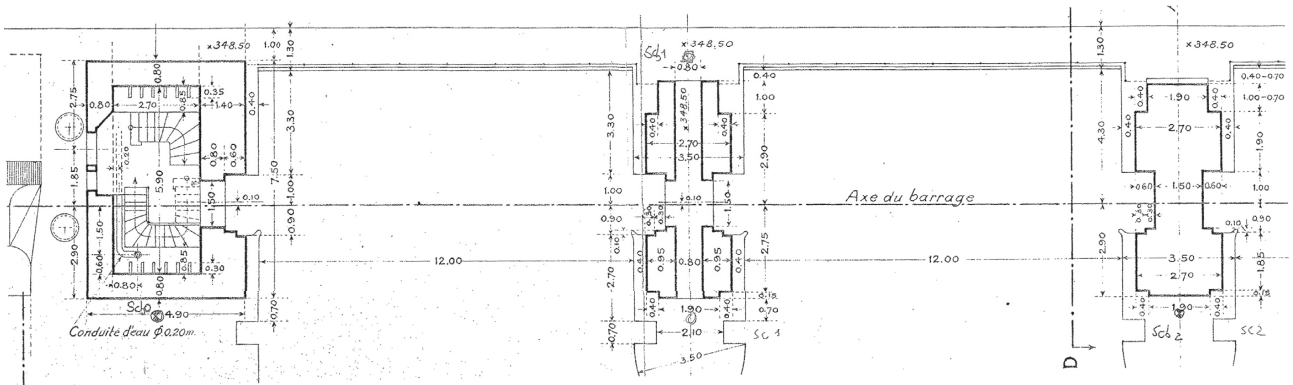


FIGURE 4: Cross sections of the cable tower, the “elephant feet” at the base, and the plain section of the piers (from left to right).

capacity. Furthermore, the displacement-based approach is very favorable for the upper bridge of the Chancy-Pouigny dam because of its relatively high stiffness, leading to a small displacement demand (Figure 8).

3.1. Assumptions. The capacity curves of the piers are determined based on the three following parameters: the top

displacement when uplift appears at the base, considered as yielding displacement, the lateral strength corresponding to a rocking failure mode, and the ultimate drift. The stiffness is the inverse ratio of the uplift displacement to the associated lateral strength. Lateral strength by rocking constitutes the plateau of the capacity curve.

The yielding displacement of the capacity curve corresponds to the top displacement at the onset of base uplift. The

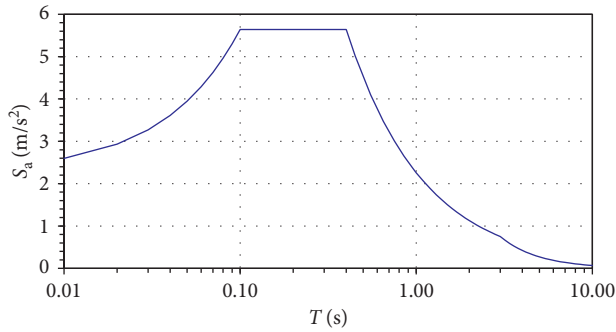


FIGURE 5: OFEN elastic response spectrum for a return period of 5000 years, soil class A, and 5% damping ratio.

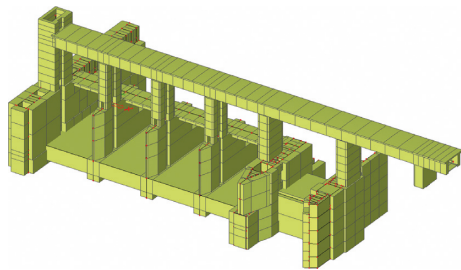


FIGURE 6: 3D finite element model of the Chancy-Pougny dam [8].

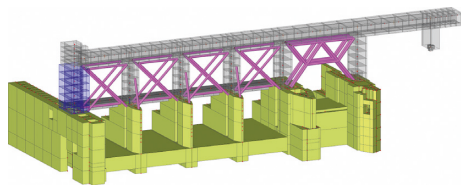


FIGURE 7: Initial proposed retrofitting solution with the huge bracing system for the upper bridge [8].

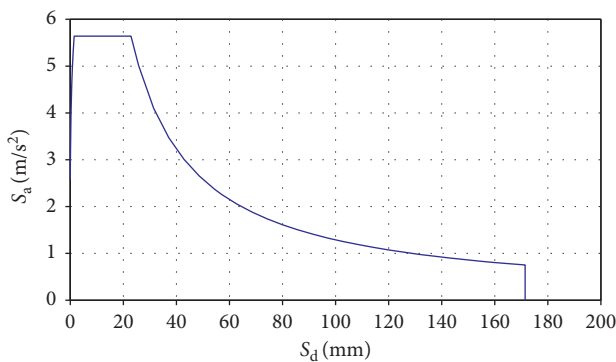


FIGURE 8: OFEN response spectrum represented in the ADRS format.

top displacement when uplift appears at the base is determined based on a model of vertical cantilever with a constant stiffness along the height by applying the basic relationships of structural mechanics (Figure 9). The considered inertia moment for the determination is that of the element's base,

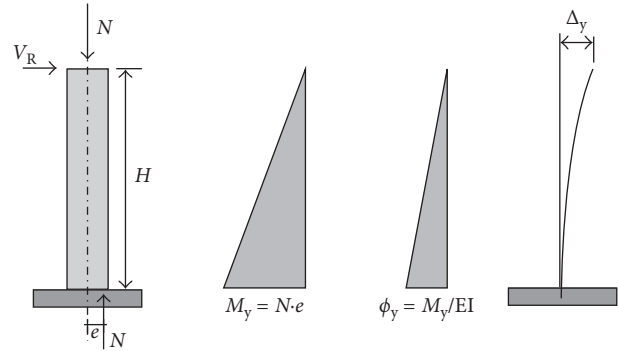


FIGURE 9: Determination of the top displacement at the onset of uplift (yielding displacement).

leading to an overestimation of the displacement because the piers are hollowed only at their base. With the displacement-based method, this assumption is, here, on the safe side because it leads to an underestimation of the stiffness. Therefore, this leads to an overestimation of the fundamental period and, consequently, to an overestimation of the displacement demand.

Based on the values of deformation capacity for masonry shear walls proposed by Eurocode 8 [13] (i.e., 0.4% in case of shear failure and 0.8% for rocking failure), a value of 0.8% was considered as ultimate drift. The very low reinforcement (near zero reinforcement) at the base of the piers leads to a rocking behavior characterized by a bending strength due to the normal compression force at the base only. Note that the adopted value for ultimate drift may be considered as very conservative because EC 8 allows for the masonry shear walls governed by a rocking failure mode to increase the basic value of 0.8% through its multiplication by the corresponding slenderness ratio.

Concerning the mechanical properties of the reinforced concrete, the dynamic characteristic values measured on samples taken on the elements are involved. For the piers, the values are:  $f_{ck} = 45$  MPa for the compressive strength and  $E_c = 46600$  MPa for Young's modulus. The cable tower concrete is of lower quality. The values are therefore lower:  $f_{ck} = 21$  MPa for the compressive strength and  $E_c = 36,200$  MPa for Young's modulus. The element stiffness is reduced to 25% when considering cracking.

**3.2. Results of the "Push-Over" Analysis.** The results of the "push-over" analysis are briefly reported here in order to provide the basis of the comparison with the nonlinear time-history analysis, which is the main objective of the paper.

Figure 10 shows the capacity curve of the upper bridge in the cross-stream direction for the current state (without retrofitting). In this direction, the upper bridge is analyzed globally because the connection by the gallery deck leads to an identical top displacement for all elements. The total mass is 4300 tons and includes the deck, the related equipments, and half the height of the piers and the cable tower. The individual curves for each element (cable tower and piers I to

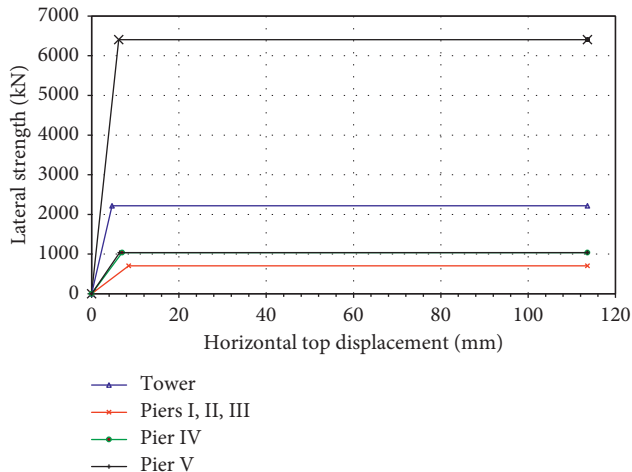


FIGURE 10: Capacity curve of the upper bridge for the cross-stream direction [9].

V) are first determined. The global capacity curve is obtained by adding up all individual curves.

In the cross-stream direction, lateral strength of the upper bridge is about 6400 kN. The yielding displacement at the top is approximately 6 mm. The fundamental period is about 0.4 s. According to the assumption of a value for ultimate drift of 0.8%, the top displacement capacity is approximately 110 mm. Note that this value is relatively small in comparison to the dimensions of the piers (Table 1).

In the stream direction, the piers may be analyzed independently because, in this direction, the connection by the gallery does not lead to an identical top displacement for the elements. The piers resist in their larger cross-sectional dimension. Therefore, the fundamental periods are much smaller than the ones in the cross-stream direction and do not exceed 0.2 s.

Figure 11 shows the seismic evaluation of the upper bridge for the cross-stream direction in the usual ADRS format. According to the EC 8 [14] procedure, the fundamental period is just entering the validity domain of the equal displacement rule. As a consequence, displacement demand does not depend on the strength of the structure [15]. For the fundamental period of the upper bridge, the top displacement demand is about 23 mm, which is much smaller than the considered top displacement capacity of 110 mm.

However, the seismic rocking behavior is associated with a low energy dissipation capacity which leads to an increase of the displacement demand compared to the usual behavior of reinforced concrete corresponding to the equal displacement rule. The displacement demand should therefore be increased in order to account for this amplification. An increase of about 25% of the displacement demand was proposed in the literature, based on extended numerical results [16]. The accuracy of the increase should be checked because a larger displacement demand may appear in the low period range [17]. Nevertheless, such an increase would not significantly modify the favorable conclusions for the seismic behavior of the upper bridge.

## 4. Nonlinear Time-History Analysis

The validation of the above reported results was requested by the French-Swiss supervisory authorities and consequently nonlinear time-history analyses were achieved in order to determine an accurate value of the amplification due to a low energy dissipation capacity for the rocking behavior of the upper bridge of the Chancy-Pouigny dam.

**4.1. Methodology.** The nonlinear time-history analyses are performed using equivalent single-degree-of-freedom systems (SDOF) and a specific hysteretic model, simulating an “S” shape (Figure 12). The central difference method is used to solve the equation of motion. There are 33 stationary synthetic accelerograms involved which are compatible with the prescribed response spectrum. A second series of 12 recorded accelerograms, slightly modified to match the prescribed response spectrum are also used.

In a first step, the analyses were performed by taking into account only the horizontal seismic actions. A reduced normal force at the base of the piers, resulting from a combination including vertical seismic actions, is considered afterwards in a second step in order to investigate the influence of the vertical accelerations linked to the earthquake.

**4.2. Assumptions.** The hysteretic curves of the equivalent SDOF are determined based on the capacity curves developed previously by the “push-over” analysis. The hysteretic curves are defined by the three following parameters: the top displacement when uplift appears at the base (considered as the “yielding” displacement), the lateral strength corresponding to a rocking failure mode, and the “postyield” stiffness. In order to be conservative, a stiffness of only 1% of the initial stiffness (before uplift) is considered for the “postyield” stiffness. The classical value of 5% for the viscous damping ratio is used.

The fixed level is assumed to be at the upper level of the pillars situated in the lower part of the dam because the pillars are much more stiff than the piers of the upper bridge. Consequently, the analyses with equivalent SDOF do not account for the pillar displacements in the lower part of the dam during the earthquake. The displacements at the upper level of the pillars should therefore be added to obtain the total displacements. However, the results of the initial force-based analyses have shown that these displacements are small compared to the ones expected for the piers and may therefore be neglected.

**4.3. Time-Histories Series.** Two series of accelerograms are used to achieve the nonlinear time-history analyses. Stationary synthetic accelerograms, compatible with the prescribed response spectrum and specified by the Swiss supervisory body [18] are involved for the first series (Figure 13). Those synthetic accelerograms were generated using the well-known classical simulation procedure of SIMQKE [19] which is a stationary simulation based on random vibration theory. In this simulation procedure,

TABLE 1: Characteristics of the piers (without taking into account the earthquake vertical component).

Element	$L$ (m)	$b$ (m)	$N$ (kN)	Cross-stream direction			Stream direction		
				$e_N$ (m)	$M_y$ (kNm)	$V_R$ (kN)	$e_N$ (m)	$M_y$ (kNm)	$V_R$ (kN)
Cable tower	7.5	4.9	15000	2.10	31500	2218	3.35	50250	3539
Piers I, II, and III	6.8	2.7	8000	1.25	10000	704	3.20	25600	1803
Piers IV and V	6.8	3.2	9500	1.55	14725	1037	3.30	31350	2208

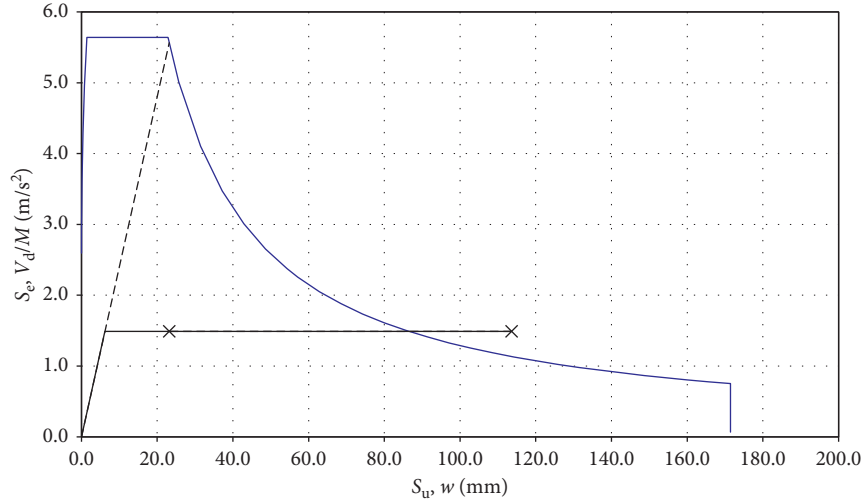


FIGURE 11: Seismic assessment of the upper bridge for the cross-stream direction [9].

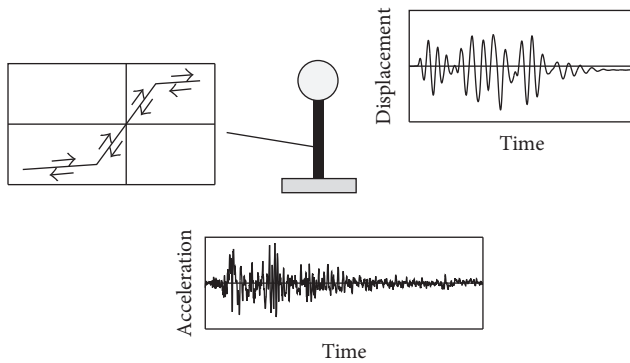


FIGURE 12: Schematic description of the performed nonlinear time-history analysis [9].

matching of the target spectrum is improved through an iterative process. However, this iterative process for matching the target spectrum was found to affect the related computed seismic structural response in case of nonlinear behavior [20]. In total, 33 accelerograms with different durations were used. The stationary durations range from 12 to 30 seconds with a step of 2 seconds. Three statistically independent accelerograms representing the three components of the earthquake shaking are specified for each stationary duration.

Since synthetic earthquake characteristics may significantly diverge from those of real earthquakes and may therefore affect the nonlinear seismic structural behavior [20], analyses are also achieved with a set of 12 recordings. These 12 recordings were first selected from the European Strong

Motion Database (ESMD) [21] to best fit the OFEN design response spectra (Figures 14 and 15). Afterwards, the selected recordings were slightly modified using the nonstationary spectral matching methodology of Abrahamson [22] in order to match the OFEN design spectrum (Figures 16 and 17). The methodology proposed by Abrahamson [22] involves wavelets to match the target spectrum without disturbing the nonstationary features of the recordings. Consequently, the related computed seismic structural response is not significantly affected even in case of nonlinear behavior.

**4.4. Results with Stationary Time-Histories.** The results of the nonlinear time-history analyses are assessed statistically by considering the mean value and the standard deviation. All the 33 time-histories are considered globally disregarding the related duration.

The obtained results for the cross-stream direction are displayed in Figure 18. For the analysis in this direction, the period of the equivalent SDOF is about 0.4 s and the yielding displacement is 6.2 mm. The computed displacement demands are plotted with respect to the duration. The three points for each duration correspond to the three components of the OFEN database. This plot shows that no clear trend appears in relation with the duration. This finding led to the aggregation of the results without taking into account the related duration. The mean value of the top displacement demand is approximately 33 mm and the peak value is approximately 42 mm. Note that even this maximum displacement demand is clearly smaller than the assumed displacement capacity. According to push-over

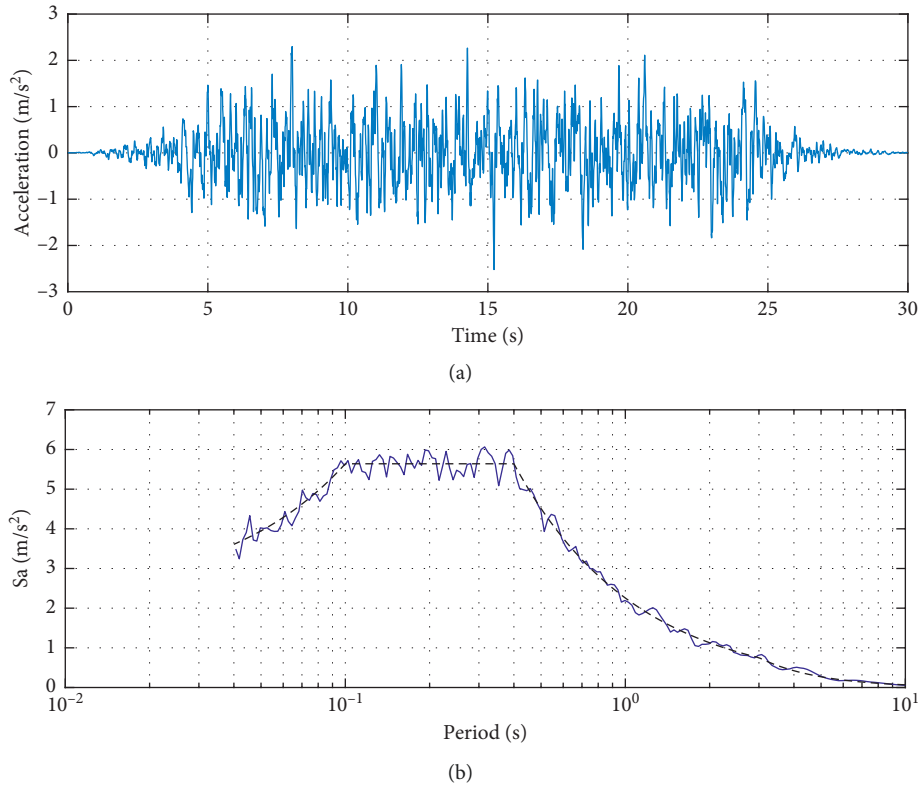


FIGURE 13: Acceleration time-history and corresponding response spectrum of one of the 33 synthetic earthquakes with a stationary duration of 18 seconds.

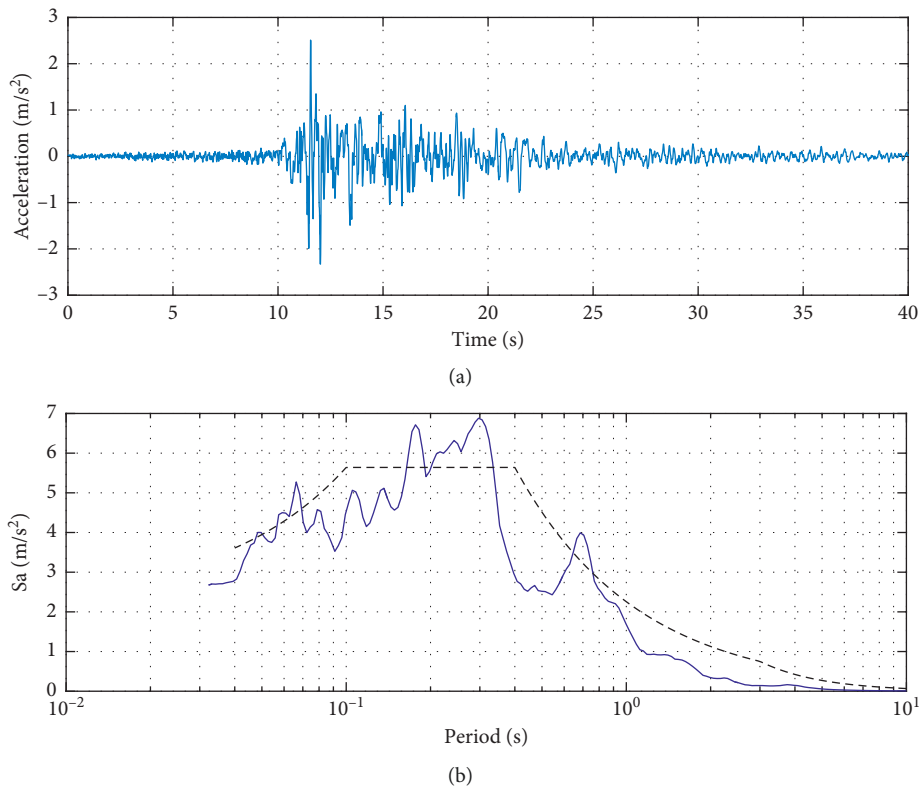


FIGURE 14: Acceleration time-history and corresponding response spectrum of a selected example among the twelve recorded earthquakes before modification to match the OFEN response spectrum.



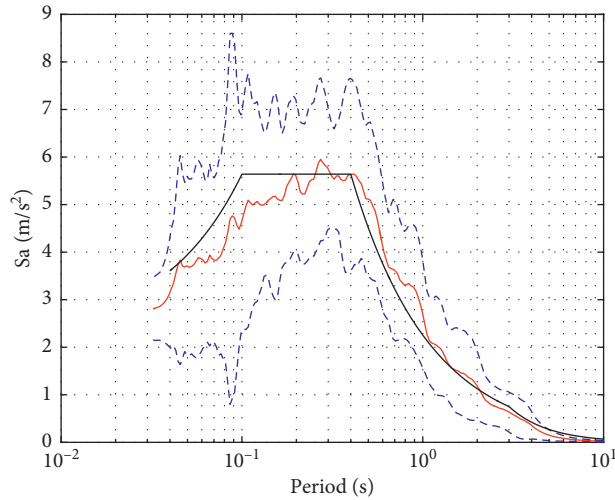


FIGURE 15: Statistical characteristics (mean value  $\pm$  standard deviation) of the response spectra of the twelve recorded earthquakes before modification to match the OFEN response spectrum.

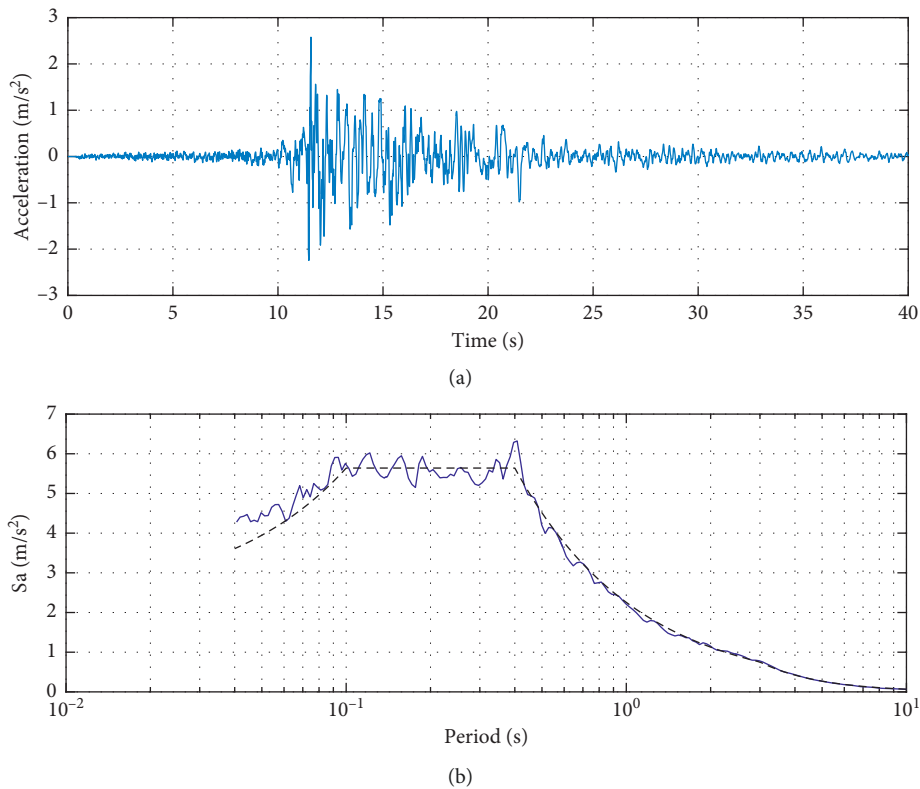


FIGURE 16: Acceleration time-history and corresponding response spectrum of the selected example among the twelve recorded earthquakes after modification to match the OFEN response spectrum.

analysis, the top displacement demand is about 23 mm (Figure 11). Thus, the statistical properties of the results indicate a larger increase of the displacement demand than the one proposed in the literature [16], with a magnitude of more than 40% for mean values. This relative larger increase than the one proposed in the literature is mainly due to the involvement of stationary synthetic time-histories which simulate only approximately the features of measured recordings.

The results of the analysis of the three identical piers (I, II, and III) in the stream direction with the 33 stationary time-histories are plotted in Figure 19. For the analysis in this direction, the period of the equivalent SDOF is approximately 0.21 s and the yielding displacement is 3.7 mm. The computed displacement demands are plotted with respect to the duration. Once again, the plot does not show a clear trend with the duration. The mean value of the top displacement demand is approximately 10 mm and the peak

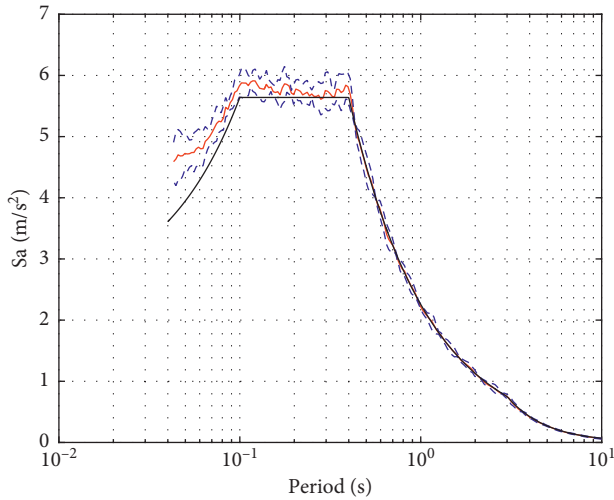


FIGURE 17: Statistical characteristics (mean value  $\pm$  standard deviation) of the response spectra of the twelve recorded earthquakes after modification to match the OFEN response spectrum.

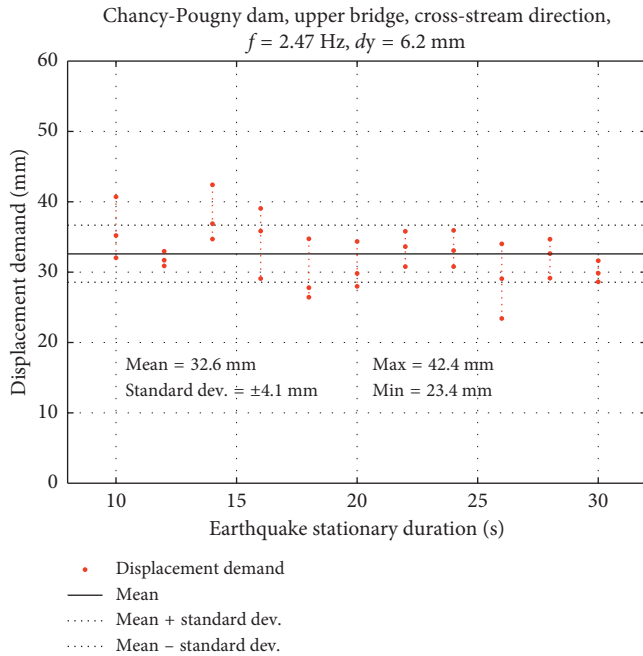


FIGURE 18: Displacement demand according to the nonlinear time-history analysis in the cross-stream direction with the 33 synthetic earthquakes.

value is approximately 19 mm. According to push-over analysis, the top displacement demand was roughly 9 mm. Therefore, in this case, the statistical properties of the results indicate limited amplifications of the displacement demand corresponding to those of the literature [16]. Moreover, this direction is not significant because the smaller fundamental periods are related to a much smaller displacement demand than those in the cross-stream direction.

4.5. Results with the Set of 12 Recorded Time-Histories. For the case of the analysis with the recorded earthquakes in the cross-stream direction, the results are displayed in

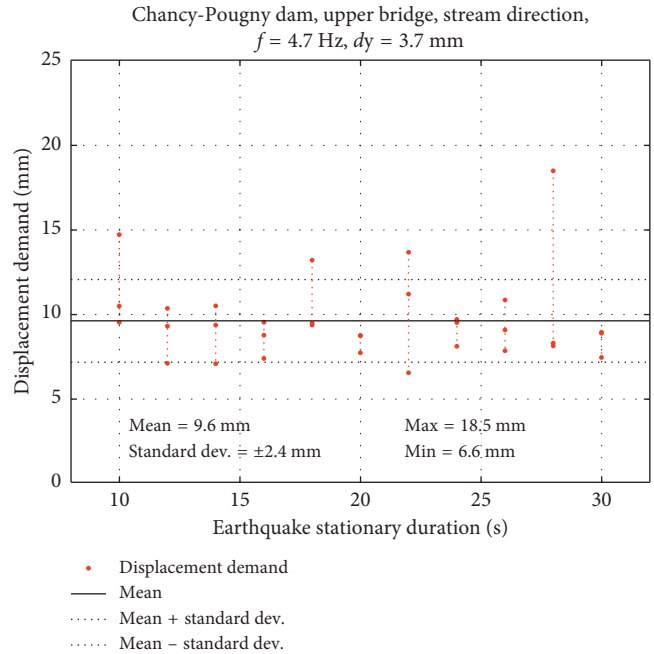


FIGURE 19: Displacement demand according to the nonlinear time-history analysis in the stream direction for the identical piers I, II, and III with the 33 synthetic earthquakes.

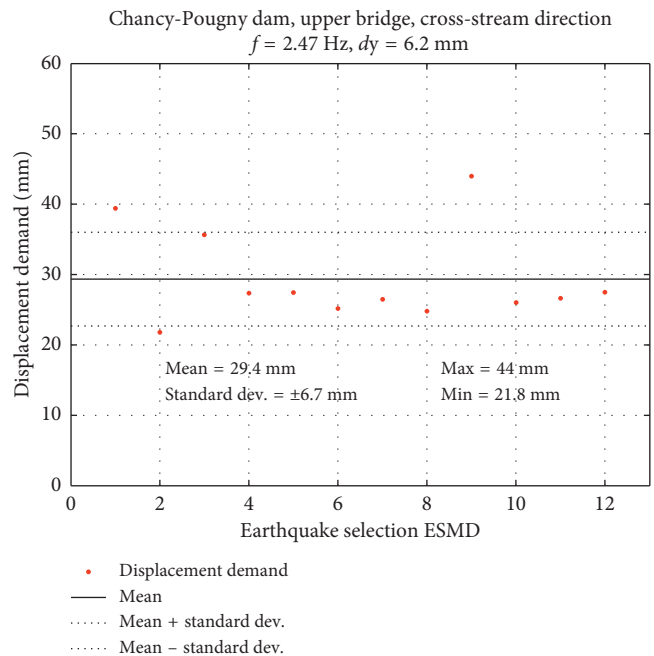


FIGURE 20: Displacement demand according to the nonlinear time-history analysis in the cross-stream direction with the set of 12 recorded earthquakes.

Figure 20. The computed displacement demands are plotted individually for each time-history. The results are very similar to those found in the analysis of the 33 synthetic earthquakes (Figure 18). The mean value of the top displacement demand is approximately 29 mm, and the peak value is 44 mm. It should be noted that even this maximum displacement demand is again clearly smaller than the

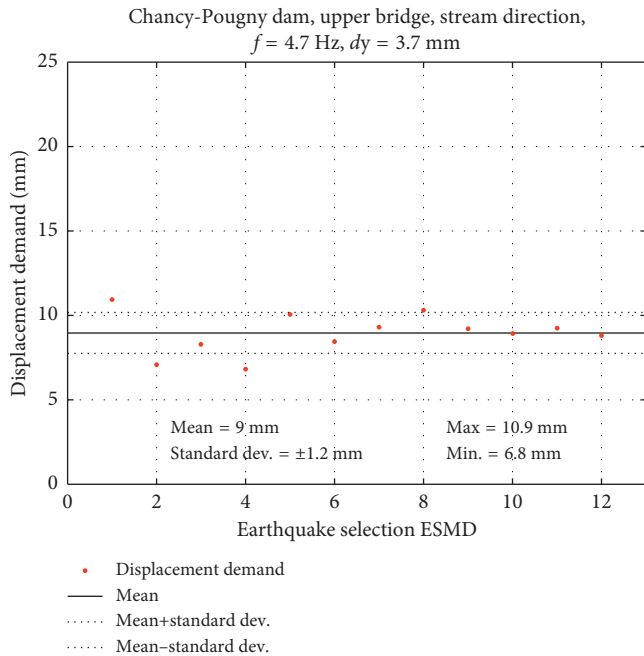


FIGURE 21: Displacement demand according to the nonlinear time-history analysis in the stream direction for the identical piers I, II, and III with the set of 12 recorded earthquakes.

displacement capacity. The statistical properties of the results indicate an increase of the displacement demand close to that proposed in the literature [16], with a value of about 28% for the mean values. This issue clearly indicates the importance of involving nonstationary time-histories to realistically capture the nonlinear seismic response.

Finally, for the analysis in the stream direction, the attained results are plotted in Figure 21. In comparison to the results for the 33 synthetic earthquakes (Figure 19), the results are similar, however with significantly smaller variability. A peak value of less than 11 mm was obtained. The statistical properties of the results indicate another time limited amplification of the displacement demand corresponding to those specified in the literature [16].

**4.6. Results with Reduced Normal Force.** In order to investigate the influence of the vertical earthquake component on the seismic behavior of the upper bridge using a simplified approach, reduced values of compressive forces ( $N_{red}$ ) at the piers' base are also considered (Table 2). The transient behavior of the vertical seismic action relative to the horizontal action is not known a priori. An approach as proposed to account for vertical earthquake component leads to results on the safe side because peak vertical acceleration is considered during the whole time-history analysis. The decrease of the compression force leads to a lower lateral strength and, therefore a lower corresponding yielding displacement. However, in the adopted model, the fundamental frequency is not affected by the decrease of the compressive forces at the piers' base because the stiffness remains constant. In the case of nonlinear behavior where "yielding" appears sooner, lower

lateral strength is generally related with an increase of displacement demand.

The impact of the vertical earthquake component on the compressive forces at the piers' base was evaluated based on the results of the 3D model (Figure 3). A related variation of the compressive forces of approximately  $\pm 20$  to 30% was attained. Consequently, the nonlinear time-history analyses are repeated with the 33 synthetic earthquakes using hysteretic curves reduced by 30% for both the yielding displacement and the strength. The obtained results allow to assess the additional increase of the displacement demand due to the reduction of the compressive forces at the piers' base.

In the cross-stream direction, the mean value of the top displacement demand is 37 mm, and the peak value is approximately 49 mm. Reduced compressive forces at the piers' base lead then to an additional increase of the displacement demand of less than 15% for the mean values. Note that, in this direction, according to the push-over analysis, the top displacement demand remains at approximately 23 mm because this value is not affected by a decrease of strength. This is due to the fact that the fundamental period belongs to the validity domain of the equal displacement rule (Figure 11).

In the stream direction, the mean value of the top displacement demand and the peak value are approximately 14 mm and 20 mm, respectively. In this direction, the impact of the reduced compressive forces at the piers' base is relatively larger than in the cross-stream direction. For the mean values, the displacement demand experiences an additional increase of almost 50%.

**4.7. Overview of the Results.** Table 3 summarized the obtained results of the different nonlinear time-history analyses. The statistical characteristics are given with one digit after the decimal point in order to facilitate the comparison of the values. Compared to the assumed conservative displacement capacity of about 110 mm, all the obtained values are significantly less, by a factor greater than 2, at least. Due to the arrangement of the elements in their larger dimension, the stream direction is less significant than the cross-stream direction.

Concerning the impact of the involved time-histories, no significant discrepancies appear between synthetic earthquakes and recorded earthquakes. Moreover, unlike other investigations in the literature [20], these findings show that recorded earthquakes lead to a slightly lower mean displacement demand.

Compared to push-over analysis, the increase of the top displacement demand due to the specific hysteretic behavior with small energy dissipation is in some cases slightly larger than that which is proposed in the literature [16], by more than 40% for the mean values.

In this study, the assumed displacement capacity was based on the value of ultimate drift (0.8%) proposed by Eurocode 8 [13] for masonry shear walls in the case of seismic behavior controlled by in-plane rocking failure. Compared to the dimensions of the cross section of the piers, the related assumed top displacement capacity of

TABLE 2: Characteristics of the piers for the cross-stream direction considering the vertical component.

Element	$L_w$ (m)	$b_w$ (m)	$e_N$ (m)	Without vertical component			With vertical component		
				$N$ (kN)	$M_y$ (kNm)	$V_R$ (kN)	$N_{red}$ (kN)	$M_y$ (kNm)	$V_R$ (kN)
Cable tower	7.5	4.9	2.10	15000	31500	2218	10900	22890	1612
Piers I, II, and III	6.8	2.7	1.25	8000	10000	704	6700	8375	590
Piers IV and V	6.8	3.2	1.55	9500	14725	1037	7600	11780	830

TABLE 3: Statistical characteristics of the obtained displacement demand at the top of the piers.

Direction	33 synthetic			12 recorded			Reduced compression		
	Mean (mm)	Std. (mm)	Max (mm)	Mean (mm)	Std. (mm)	Max (mm)	Mean (mm)	Std. (mm)	Max (mm)
Cross-stream	32.6	4.1	42.4	29.4	6.7	44.0	37.0	5.6	48.6
Stream (piers I to III)	9.6	2.4	18.5	9.0	1.2	10.9	14.2	3.1	20.4

approximately 110 mm may appear excessively conservative. Precisely, larger displacement capacities are usually considered for rigid body seismic behavior, such as the ones involved for out-of-plane behavior of unreinforced masonry walls [23, 24]. Theoretically, top displacements which are larger than the lateral width of the rocking rigid body element should be reached to attain collapse. Consequently, the displacement capacity corresponding to a portion of the width (e.g., 50%) could be considered. However, since the results of this study were already satisfactory with the assumed displacement capacity, it was not necessary to improve this assumption.

## 5. Conclusions

The performed nonlinear time-history analyses fully validate the favorable results obtained by push-over analysis. The displacement-based approach is very favorable for the upper bridge of the Chancy-Pougny dam because of its relatively high stiffness, leading to a small displacement demand. In contrast to previous displacement-based analyses, accurate values of the amplification due to a low energy dissipation capacity for the rocking behavior of the upper bridge of the Chancy-Pougny dam could be determined. Even if the increase of the top displacement demand due to the specific hysteretic behavior with small energy dissipation is in some cases larger than that proposed in the literature, the displacement demands remain far lower than the assumed conservative displacement capacity.

Consequently, the initially proposed very invasive measure for the upper bridge with a huge bracing system could be eliminated from the retrofitting project. This would lead to a significant benefit for the assessment of the Chancy-Pougny dam, not only from the cost point of view but also from the monumental preservation point of view. Instead of avoiding cracking at the base, this failure mode may be used since the reported investigations prove that it leads to a seismically satisfactory rocking behavior which is associated with a displacement capacity much larger than the displacement demand. However, in order to ensure that the upper bridge will behave without local failures, additional checks and some local measures are still necessary. First of all, it was verified that shear failures may be excluded at the base of the piers. The so-called “elephant feet” (Figure 4) at

TABLE 4: Characteristics of the 12 recorded earthquakes.

Earthquake	Date	Magnitude	Distance (km)	PGA ( $m/s^2$ )
Azores	23/11/1973	5.3 Ms	5	2.688
Friuli (aftershock)	15/09/1976	6.0 Mw	17	2.319
Montenegro (aftershock)	24/05/1979	6.2 Mw	33	2.652
Adana	27/06/1998	6.3 Mw	30	2.644
Montenegro	15/04/1979	6.9 Mw	65	2.509
Montenegro	15/04/1979	6.9 Mw	21	2.198
Campano Lucano	23/11/1980	6.9 Mw	16	1.725
Alkion	24/02/1981	6.6 Mw	33	3.036
Tabas	16/09/1978	7.4 Mw	11	3.779
Izmit	17/08/1999	7.6 Mw	113	2.58
Izmit	17/08/1999	7.6 Mw	48	2.334
Izmit	17/08/1999	7.6 Mw	34	3.542

the base of the identical piers (I, II, and III) are of utmost concern. However, due to the relatively high slenderness (height/length ratio) of the four squat columns composing the “elephant feet” (length of about 1 to 2 m), the base shear may be directly transferred to the upper part of the pillars through inclined compression stress fields, without additional shear contribution. Piers IV, V, and the cable tower are even less prone to shear failure because of their hollow cross section at the base. The main local retrofitting measure is situated at the top of the piers where steel elements will be placed inside the deck of the upper bridge in order to avoid the falling of the simply supported beams during the rocking behavior. Additionally, the abutment on the right bank slope should be stabilized in the cross-stream direction by post-tensioned ground anchors.

## Appendix

The characteristics of the 12 recorded earthquakes involved in the study are summarized in Table 4.

## Data Availability

The data used to support the findings of this study are available from ResearchGate (<https://www.researchgate.net/publication/>

326294022\_Acceleration\_Time-Histories\_DATA) and from the corresponding author upon request

## Conflicts of Interest

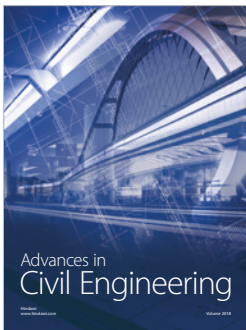
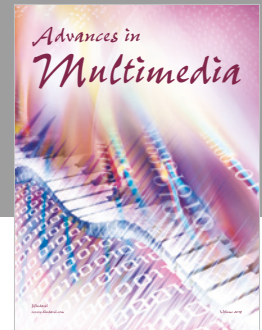
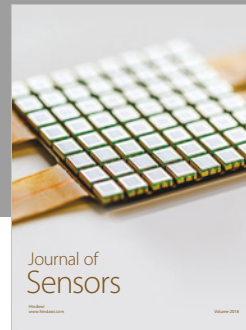
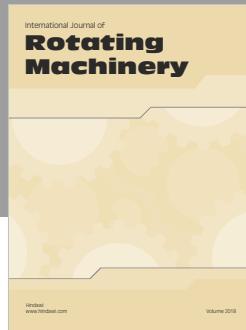
The authors declare that they have no conflicts of interest.

## Acknowledgments

The investigations were funded by the Société des Forces Motrices de Chancy-Pougny (SFMCP). The Swiss Federal Office of Energy (OFEN) and the Direction Régionale de l'Environnement, de l'Aménagement et du Logement (DREAL) supervised the project. Comments and suggestions from the supervisory authorities expert, Olivier Vallotton from Stucky SA in Renens, Switzerland, are deeply appreciated.

## References

- [1] M. J. N. Priestley, "Myths and Fallacies in Earthquake Engineering Revisited," in *The Mallet Milne Lecture*, Istituto Universitario di Studi Superiori di Pavia, Pavia, Italy, 2003.
- [2] G. M. Calvi, "A displacement-based approach for vulnerability evaluation of classes of buildings," *Journal of Earthquake Engineering*, vol. 3, no. 3, pp. 411–438, 1999.
- [3] T. Paulay and M. N. J. Priestley, *Seismic Design of Reinforced Concrete and Masonry Buildings*, ISBN: 0-471-54915-0, John Wiley & Sons, Hoboken, NJ, USA, ISBN: 0-471-54915-0, 1992.
- [4] J. P. Moehle, "Displacement-based design of RC structures subjected to earthquakes," *Earthquake Spectra*, vol. 8, no. 3, pp. 403–428, 1992.
- [5] M. J. N. Priestley, G. M. Calvi, and M. J. Kowalsky, *Displacement-Based Seismic Design of Structures*, IUSS Press, Pavia, Italy, 2007.
- [6] E. G. Dimitrakopoulos and M. J. DeJong, "Overturning of retrofitted rocking structures under pulse-type excitations," *Journal of Engineering Mechanics ASCE*, vol. 138, no. 8, pp. 963–972, 2012.
- [7] M. A. ElGawady and A. Sha'Ian, "Seismic behavior of self-centering precast segmental bridge bents," *Journal of Bridge Engineering*, vol. 16, no. 3, pp. 328–339, 2011.
- [8] J. P. Person, M. Ferrière, and H. Charif, "Seismic Reinforcement of Chancy-Pougny Dam," in *Proceedings of the Hydro 2010 International Conference*, Lisbon, Portugal, September 2010.
- [9] M. Ferrière, J. P. Person, H. Charif, O. Vallotton, S. Rossier, and P. Lestuzzi, "Seismic Safety of Chancy-Pougny Dam," in *Proceedings of the Symposium of the 79th ICOLD Annual Meeting*, Lucerne, Switzerland, June 2011.
- [10] P. Lestuzzi and M. Badoux, *Evaluation Parasismique des Constructions Existantes*, ISBN 978-2-88074-990-3, Presses Polytechniques et Universitaires Romandes, Lausanne, Switzerland, ISBN 978-2-88074-990-3, 2013.
- [11] OFEN prescriptions, in *Sécurité des Ouvrages d'Accumulation. Documentation de Base Pour la Vérification des Ouvrages d'accumulation Aux Séismes, Dam Security. Basic Documentation for the Seismic Assessment of Dams, version 1.2*, 2003, in French and German.
- [12] C. Greifenhagen and P. Lestuzzi, "Static-cyclic tests on low reinforced concrete shear walls," *Engineering Structures*, vol. 27, no. 11, pp. 1703–1712, 2005.
- [13] Eurocode 8, *Design of Structures for Earthquake Resistance-Part 3: Assessment and Retrofitting of Buildings*, European Committee for Standardization, Brussels, Belgium, 2005.
- [14] Eurocode 8, *Design of Structures for Earthquake Resistance-Part 1: General Rules, Seismic Actions and Rules for Buildings*, European Committee for Standardization, Brussels, Belgium, 2004.
- [15] P. Lestuzzi and M. Badoux, "An Experimental Confirmation of the Equal Displacement Rule for RC Structural Walls," in *Proceedings of the Fib-Symposium: Concrete Structures in Seismic Regions*, Athens, Greece, May 2003.
- [16] P. Lestuzzi, Y. Belmouden, and M. Trueb, "Non-linear seismic behavior of structures with limited hysteretic energy dissipation capacity," *Bulletin of Earthquake Engineering*, vol. 5, no. 4, pp. 549–569, 2007.
- [17] C. Michel, P. Lestuzzi, and C. Lacave, "Simplified non-linear seismic displacement demand prediction for low period structures," *Bulletin of Earthquake Engineering*, vol. 12, no. 4, pp. 1563–1581, 2014.
- [18] OFEN report, in *Beschleunigungszeitverläufe in Übereinstimmung Mit der BWG Richtlinie zur Erdbebensicherheit von Stauanlagen, Acceleration Time-Histories According to the BWG Prescriptions for Seismic Security of Dams*, 2003, German.
- [19] D. A. Gasparini and E. H. Vanmarcke, "Simulated earthquake motions compatible with prescribed response spectra," MIT Civil Engineering Research Report R76–4, Massachusetts Institute of Technology, Cambridge, MA, USA, 1976.
- [20] P. Schwab and P. Lestuzzi, "Assessment of the non-linear seismic behavior of ductile wall structures due to synthetic earthquakes," *Bulletin of Earthquake Engineering*, vol. 5, no. 4, pp. 67–84, 2007.
- [21] N. Ambraseys, P. Smit, R. Sigbjornsson, P. Suhadolc, and B. Margaris, *Internet-Site for European Strong-Motion Data, European Commission, Research-Directorate General, Environment and Climate Programme*, 2002.
- [22] N. A. Abrahamson, "Non-stationary spectral matching," *Seismological Research Letters*, vol. 63, no. 1, p. 30, 1992.
- [23] M. C. Griffith, N. Lam, J. Wilson, and K. Doherty, "Experimental investigation of unreinforced brick masonry walls in flexure," *ASCE Journal of Structural Engineering*, vol. 130, no. 3, pp. 423–432, 2004.
- [24] O. Al Shawa, G. De Felic, A. Mauro, and L. Sorrentino, "Out-of-plane seismic behaviour of rocking masonry walls," *Earthquake Engineering and Structural Dynamics*, vol. 41, no. 5, pp. 949–968, 2012.



**Hindawi**

Submit your manuscripts at  
[www.hindawi.com](http://www.hindawi.com)

